

# Electron counting in a silicon single-electron pump

Tuomo Tantt\*, Kuan Yen Tan, Kukka-Emilia Huhtinen, and Mikko Möttönen  
QCD Labs, COMP Centre of Excellence, Department of Applied Physics,  
Aalto University, P.O. Box 13500, 00076 Aalto, Finland

Alessandro Rossi, Kok Wai Chan,<sup>†</sup> and Andrew S. Dzurak  
School of Electrical Engineering & Telecommunications,  
The University of New South Wales, Sydney 2052, Australia  
(Dated: June 9, 2019)

We report electron counting experiments in a silicon metal–oxide–semiconductor quantum dot architecture which has been demonstrated to generate a quantized current in excess of 80 pA with uncertainty below 30 parts per million. Single-shot detection of electrons pumped into a mesoscopic reservoir is performed using a capacitively coupled single-electron transistor. We extract the full probability distribution of the transfer of  $n$  electrons per pumping cycle for  $n = 0, 1, 2, 3$ , and 4. We find that the probabilities extracted from the counting experiment are in excellent agreement with direct current measurements in a broad range of dc electrochemical potentials of the pump. The electron counting technique is also used to confirm the improving robustness of the pumping mechanism with increasing electrostatic confinement of the quantum dot.

Recent development in the field of single-charge pumping has provided a basis for the emerging quantum standard of the ampere in the International System of Units (SI)[1]. This standard will be based on an agreed value for the elementary charge  $e$  and the frequency  $f$ , the product of which yields the ampere.

Single-charge pumps and turnstiles have been implemented in many different physical systems including normal-metal tunnel junction devices [2, 3], superconducting devices [4–6], hybrid superconductor–normal-metal turnstiles [7, 8], semiconductor quantum dots [9–14], and single atom-sized impurities [15–18]. A satisfactory relative pumping accuracy at the  $10^{-8}$  level has only been demonstrated in normal-metal devices in the picoampere range [2]. This current, however, falls significantly below 100 pA which is required for a practical realization of the quantum current standard [19]. The most accurate single-electron pumps that produce high enough current are thus far based on GaAs quantum dots, in which an uncertainty of 1.2 parts per million (ppm) has been reached at 150-pA current [20, 21].

Silicon quantum dots [11, 13, 22–24] provide a promising alternative to the GaAs platform. Devices based on silicon have greatly suppressed  $1/f$  noise and absence of large amplitude background charge jumps [25]. To date the most accurate silicon single-electron pumps produce a pumped current of 80 pA with uncertainty below 30 ppm [13].

The accuracy of the electron pump is essentially given by missed or excess electrons pumped per cycle. It is possible to arrange the electron pumps such that the pumping errors can be in-situ observed with a nearby charge sensor, thus providing a self-referenced current source.

Although several experiments [2, 17, 22, 26–29] provide observations on the pumping errors and the number of electrons transferred per cycle, a thorough comparison of the direct current provided by the electron pump and the results of the electron counting scheme is lacking. Only comparison between electron counting and the current flowing through a non-driven system has been reported [30].

In this paper, we demonstrate electron counting in a silicon electron pump utilizing the quantum dot architecture which has provided the most accurate results in silicon [13], thus providing a proof of concept for a self-referenced silicon charge pump. Furthermore, the average number of pumped electrons per cycle,  $n$ , extracted from our electron counting scheme equals that obtained from the pumped direct current. This result verifies the consistency between these two schemes.

Our device shown in Figs. 1(a) and 1(c) is fabricated using metal–oxide–semiconductor (MOS) technology on a near-intrinsic silicon substrate with 8-nm thermally grown  $\text{SiO}_2$  gate-oxide [13]. The aluminum gates are defined with electron beam lithography in three layers isolated from each other by thermally grown  $\text{Al}_y\text{O}_x$ . The topmost layer of gates is used to accumulate a two-dimensional electron gas (2DEG) at the Si/ $\text{SiO}_2$  interface and the two bottom layers are used to control the electrostatic confinement of the dot in the planar directions by locally depleting the 2DEG and forming tunnel barriers. A schematic potential landscape of the device is presented in Fig. 1(b).

We employ two different measurement schemes: the *direct-current scheme* and the *electron counting scheme*. In the direct-current scheme, we induced a 2DEG below the source lead (SL), drain lead (DL), and switch barrier (SB) gates [see Fig. 1(a)]. The pump dot is induced with the plunger gate (PL) such that the left barrier (BL) and right barrier (BR) gates are used to define tunable tunnel barriers between the leads and the dot. The confining

\* tuomo.tanttu@aalto.fi

<sup>†</sup> Present address: Centre for Advanced 2D Materials and Graphene Research Centre, National University of Singapore

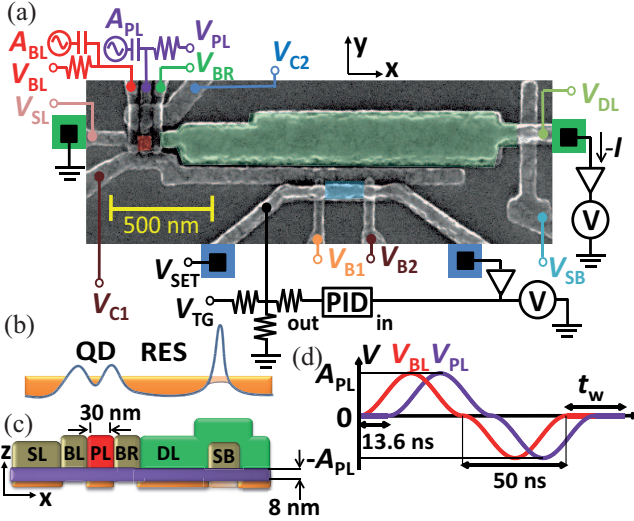


FIG. 1. (a) Scanning electron micrograph of a device in false color similar to the one used in the experiments together with a sketch of the measurement setup. The quantum dot (QD) used to pump electrons is highlighted in red. The mesoscopic reservoir (RES), into which the electrons are pumped, is green and the dot of the single-electron transistor sensor is highlighted in blue. The green (blue) squares represent the source and drain ohmic contacts of the pump (sensor). The gates are labelled according to their indicated dc voltages. (b) Schematic potential landscape of the device along  $x$ . By changing  $V_{SB}$  we can vary the reservoir to be either a large dot (electron counting scheme) or a current lead (direct-current scheme). The 2DEG is indicated with orange. The shaded area indicates 2DEG which can be induced or depleted by varying  $V_{SB}$ . (c) Schematic cross section of the device along  $x$ . (d) The repeated waveforms of the voltage drive on BL (red) and PL (purple) used in the experiment.

gates (C1 and C2) are set to negative voltage to tighten the dot potential as demonstrated in Ref. 13. Experiments in both schemes are carried out in a cryostat with a bath temperature of 180 mK.

The gates PL and BL are also connected to an arbitrary-waveform generator providing the voltage drive for the dot to pump the electrons from the source to the drain. As shown in Fig. 1(d) the waveforms of the pulses consist of three consecutive parts: (i) voltage  $s_1(t) = A_{PL/BL}[1 - \cos(2\pi t/T)]/2$  for  $0 \leq t < T$ , (ii) voltage  $s_2(t) = -s_1(2T - t)$  for  $T \leq t < 2T$ , and (iii) zero voltage for  $2T \leq t \leq 2T + t_w$ . The period of the sinusoidal part is fixed at  $T = 50$  ns and the pumping frequency  $f = 1/(2T + t_w)$  is adjusted by changing the wait time  $t_w \gg T$ . The temporal offset of the pulses in PL and BL is 13.6 ns and the voltage amplitudes at the sample are denoted by  $A_{PL}$  and  $A_{BL}$ , respectively. The induced current is measured from the drain side using a room-temperature transimpedance amplifier. In the direct-current scheme, we have  $t_w = 1.9$   $\mu$ s implying  $ef = 0.8$  pA.

The electron counting scheme has the following differ-

ences from the scheme described above: We use a much lower  $V_{SB}$  to define a mesoscopic reservoir below the DL gate bounded by SB, C1, and BR gates. The charge state of the reservoir is monitored with a capacitively-coupled single-electron transistor (SET). The SET is induced with the top gate (TG) and barrier gates (B1 and B2). The hold time of the charge state of the reservoir was measured at gate voltages similar to the one used for the counting experiments and showed stability of several hours. The current through the voltage biased SET is transimpedance amplified and channeled to a proportional-integral-derivative (PID) controller which keeps the operation point of the SET fixed by compensating  $V_{TG}$ . Electrons are pumped to the reservoir with an identical waveform as in the direct-current scheme but with relatively long wait time  $t_w = 750$  ms. After several subsequent pumping cycles, the reservoir is initialized by inducing a 2DEG below BL, PL, and BR so that the excess electrons flow from the reservoir back to the source.

Figure 2(a) shows a representative trace of the SET current signal as a function of time when electrons are pumped into the reservoir. At each pumping event, there is a clear peak in the signal which subsequently saturates back to the set point of the PID controller. The PID controller is employed to enhance the signal to noise ratio compared with the current threshold method typically used in electron counting experiments [17, 28, 29]. The advantages of our method are that the low-frequency noise is filtered out and the sensor works at its most sensitive operation point at all times. We characterize the size of each peak by the area between the SET trace and the set point as indicated in Fig. 2(a). A cumulative histogram of the SET signal areas obtained for a broad range of dc plunger gate voltages  $V_{PL}$  in the electron counting scheme is shown in Fig. 2(b). Using the data from the direct-current scheme we examine separately each operation regime, where the amount of electrons transferred per cycle is roughly an integer  $n = 0, 1, 2, 3$ , and 4. We set the threshold values for each number of electrons transferred per cycle half way between the mean values of the SET signal areas obtained from each of these operation regimes.

Figure 2(c) shows the probability of a single-electron transition as a function of applied pumping cycles before the initialization of the reservoir. The initialization process was repeated 200 times with up to 400 pumping cycles before each. The data show that we may inject at least 40 electrons into the reservoir without changing the transfer probability more than 1%. This probability decreases with increasing number of pumped electrons into the reservoir due to its increasing electrochemical potential. We estimate the capacitance between DL and the reservoir by assuming them to be parallel plate capacitors:  $C_{RES-DL} = \epsilon A/d \approx 1.8 \times 10^{-15}$  F, where  $\epsilon$  is the permittivity of  $\text{SiO}_2$ ,  $A$  is the area of the reservoir dot, and  $d$  is the thickness of the  $\text{SiO}_2$ . Thus the charging energy of the reservoir is roughly  $E_C = e^2/C_{RES-DL} \approx 87$   $\mu$ eV leading to a potential difference of the reservoir due to 40

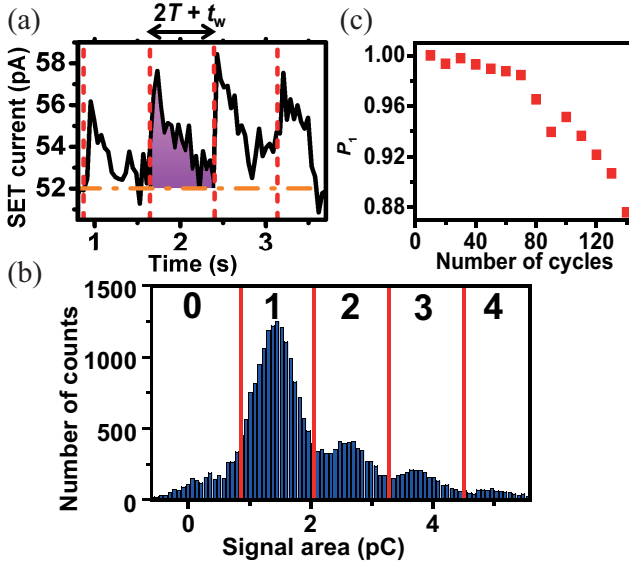


FIG. 2. (a) Representative trace of the SET signal in the electron counting experiments. The red vertical dashed lines indicate the time instants of the pumping events. The orange horizontal dashed line is the set point of the PID controller. The number of electrons transferred during the pumping cycle is estimated from the area between the set point and the SET signal as indicated. (b) Cumulative histogram of the SET signal area [shaded area in (a)] between two consecutive pump pulses with  $V_{PL}$  ranging from 0.48 V to 0.65 V. The red vertical lines show the threshold values determining the number of electrons pumped in each cycle as indicated. (c) Probability of a single electron transition as a function of the number of pumping cycles from the initialization of the reservoir. The dc values of the gates were set corresponding to one transferred electron per cycle in the direct-current scheme.

excess electrons in the island is  $\Delta_{RES} \approx 3.5$  meV. This is comparable to the charging energy of the dot  $\approx 10$  meV [13]. The success probability of pumping stays above 90% even if there are 100 excess electrons in the reservoir.

A comparison between the direct current and charge counting schemes is presented in Fig. 3(a). The probability of pumping  $k$  electrons per cycle,  $P_k$ , is obtained as a fraction of counts between the  $k$ :th and  $(k+1)$ :th threshold shown in Fig. 2(b). The average number of electrons pumped per cycle can be computed from these probabilities as  $P_\Sigma = \sum_k kP_k$ . This provides an excellent agreement with the same value extracted from the direct-current scheme  $n = I/(ef)$  for  $V_{PL} > 0.5$ . To achieve the agreement between the methods, we shifted the  $P_k$  curves by  $-8.45$  mV in  $V_{PL}$  justified by the capacitive coupling between the SB gate and the pump dot and the fact that we need to use a different gate voltage in the direct-current scheme ( $V_{SB} = 0.39$  V) compared with the charge counting scheme ( $V_{SB} = 0.20$  V). We verified that the magnitude of the applied shift is in agreement with the observed shift of the current plateaux in the direct-current scheme [see Fig. 3(b)]. The electron channel under the switch barrier turns off completely around

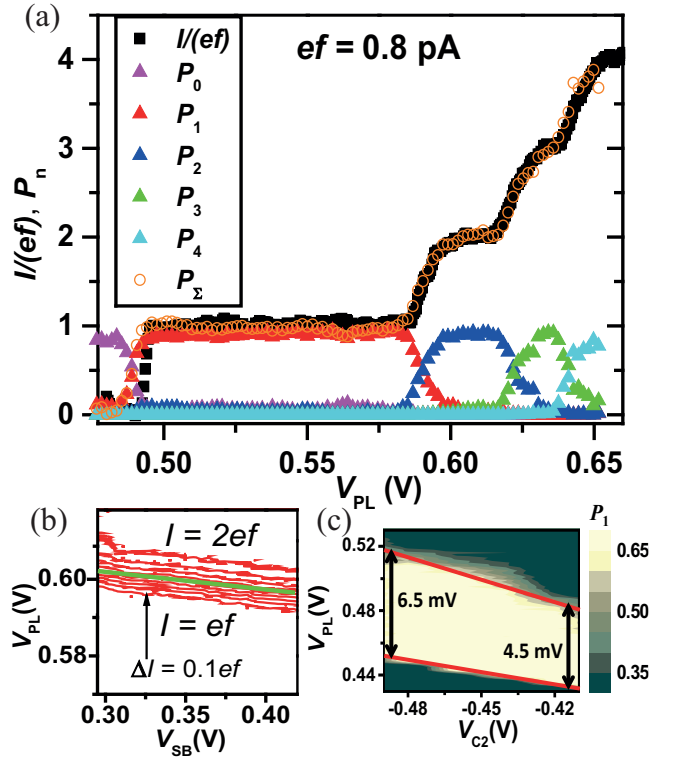


FIG. 3. (a) Measured average number of pumped electrons extracted from the pumped direct current  $n = I/(ef)$  and the probabilities  $P_k$  for different number of electrons pumped per cycle determined from the charge counting experiment as functions of the plunger gate dc voltage  $V_{PL}$ . The reservoir was initialized after every 22 pumping pulses and the initialization process was repeated 12 times for each  $V_{PL}$ . The contours of the curves from the charge counting experiment have been shifted in  $V_{PL}$  by  $-8.45$  mV to compensate the different value of  $V_{SB}$  in the two experiments. The parameters in both of these schemes were:  $V_{BL} = 0.63$  V,  $V_{BR} = 0.48$  V,  $V_{C2} = -1.0$  V,  $V_{C1} = -0.25$  V,  $V_{SL} = 2.4$  V,  $V_{DL} = 1.9$  V,  $V_{B1} = 0.85$  V, and  $V_{B2} = 0.69$  V. In the direct-current scheme we employ  $V_{SB} = 0.20$  V and  $V_{TG} = 0.98$  V, and in the charge counting scheme we have  $V_{SB} = 0.39$  V and  $V_{TG} = 0.95$  V. The amplitudes of the rf drives were  $A_{PL} = A_{BL} = 0.15$  V in both schemes. (b) Pumped direct current as a function of the plunger gate dc voltage  $V_{PL}$  and switch barrier dc voltage  $V_{SB}$ . The parameter values here are the same as in panel (a). The difference in current between the red contours is  $0.1ef$ . The green line is a guide for the eye to indicate the applied linear compensation in  $V_{PL}$  due to the different value in  $V_{SB}$ . (c) Probability of one electron transition  $P_1$  as a function of plunger and C2 gate dc voltages  $V_{PL}$  and  $V_{C2}$ . The parameter values in this experiment are the same as in (a) except for  $V_{BL} = 0.60$  V and  $V_{TG} = 1.2$  V.

$V_{SB} = 0.30$  V which prevented us from measuring the shift in this scheme at lower voltages. We neglect the shift of the plateaux due to different  $V_{TG}$  used in the two schemes since it is significantly smaller than the shift due to  $V_{SB}$ .

In the electron counting scheme the step to the first plateau shifts in  $V_{PL}$  as a function of number of ex-

cess electrons in the reservoir. Since we average over 22 pumped electrons this shift broadens the rise to the first plateau in Fig. 3(a). This effect is not clearly visible for the other, notably broad, steps. In addition, Fig. 3(a) shows that the electron counting scheme yields a slightly wider plateau for  $n = 1$  than the direct-current scheme. We attribute this difference to the voltage shift due to  $V_{SB}$ [27].

As shown in Fig. 2(b), the probability distributions of the different transitions are overlapping and consequently the probabilities are subject to a systematic error of the order 10%. The distance between two peaks is roughly 3.2 times the standard deviation of an individual peak. The overlap is due to the weak coupling between the charge detector and the reservoir leading to low signal-to-noise ratio. Note that the accuracy of the pump is significantly higher [13] than 90% which we may claim from the direct current experiment. Although the error in the probabilities is higher than in some previous electron counting experiments [17, 27, 28], our results importantly show that the probabilities extracted from the counting experiments are indeed reliable in light of the direct current experiment.

The probability of  $P_1$  in the electron counting scheme as a function of  $V_{C2}$  and  $V_{PL}$  is presented in Fig. 3(c). We observe that the width of the plateau in  $V_{PL}$  increases as  $V_{C2}$  decreases. This is due to increase in the charging energy caused by the confinement of the pump dot. Here, we show this effect in the electron counting scheme instead of direct-current scheme employed in the previous studies [13, 31].

In conclusion, we have measured the average number of

electrons pumped per cycle using both the direct current generated by the pump and a detector dot counting the number of electrons pumped in each cycle. With essentially the same experimental parameters in both of these schemes, we achieved an excellent agreement in the average pumped charge. We also verify the beneficial effect of tunable electrical confinement in the electron counting scheme. In future, we aim to strengthen the capacitive coupling between the detector dot and reservoir, to be able to perform reliable error counting in this device architecture. Ultimately, a precise electron pump verified by error counting not only provides a supreme candidate for the realization of the quantum ampere[1] but can also be harnessed in the quantum metrological triangle experiment[32, 33] to test the fundamental constants of nature.

## ACKNOWLEDGMENTS

We thank F. Hudson, C. H. Yang, Y. Sun, G. C. Tettamanzi, I. Iisakka, A. Manninen, and A. Kemppinen for useful discussions. We acknowledge financial support from the Australian Research Council (Grant No. DP120104710), the Academy of Finland (Grant No. 251748, 135794, 272806, 276528), Jenny and Antti Wihuri Foundation, The Finnish Cultural Foundation, and the Australian National Fabrication Facility. We acknowledge the provision of facilities and technical support by Aalto University at Micronova Nanofabrication Centre. A.R. acknowledges support from the University of New South Wales Early Career Researcher Grant scheme.

- 
- [1] J. Pekola, O.-P. Saira, V. Maisi, A. Kemppinen, M. Möttönen, Y. Pashkin, and D. Averin, *Rev. Mod. Phys.* **86**, 1421 (2013).
  - [2] M. W. Keller, J. M. Martinis, N. M. Zimmerman, and A. H. Steinbach, *Appl. Phys. Lett.* **69**, 1804 (1996).
  - [3] M. W. Keller, A. L. Eichenberger, J. M. Martinis, and N. M. Zimmerman, *Science* **285**, 1706 (1999).
  - [4] L. J. Geerligs, S. M. Verbrugh, P. Hadley, J. E. Mooij, H. Pothier, P. Lafarge, C. Urbina, D. Esteve, and M. H. Devoret, *Z. Phys. B* **85**, 349 (1991).
  - [5] J. J. Vartiainen, M. Möttönen, J. P. Pekola, and A. Kemppinen, *Appl. Phys. Lett.* **90**, 082102 (2007).
  - [6] M. Möttönen, J. J. Vartiainen, and J. P. Pekola, *Phys. Rev. Lett.* **100**, 177201 (2008).
  - [7] J. P. Pekola, J. J. Vartiainen, M. Möttönen, O.-P. Saira, M. Meschke, and D. V. Averin, *Nature Phys.* **4**, 120 (2008).
  - [8] V. F. Maisi, O.-P. Saira, Y. A. Pashkin, J. S. Tsai, D. V. Averin, and J. P. Pekola, *Phys. Rev. Lett.* **106**, 217003 (2011).
  - [9] L. P. Kouwenhoven, A. T. Johnson, N. C. van der Vaart, C. J. P. M. Harmans, and C. T. Foxon, *Phys. Rev. Lett.* **67**, 1626 (1991).
  - [10] M. D. Blumenthal, B. Kaestner, L. Li, S. Giblin, T. J. B. M. Janssen, M. Pepper, D. Anderson, G. Jones, and D. A. Ritchie, *Nature Phys.* **3**, 343 (2007).
  - [11] K. W. Chan, M. Möttönen, A. Kemppinen, N. S. Lai, K. Y. Tan, W. H. Lim, and A. S. Dzurak, *Appl. Phys. Lett.* **98**, 212103 (2011).
  - [12] X. Jehl, B. Voisin, T. Charron, P. Clapera, S. Ray, B. Roche, M. Sanquer, S. Djordjevic, L. Devoille, R. Wacquez, and M. Vinet, *Phys. Rev. X* **3**, 021012 (2013).
  - [13] A. Rossi, T. Tanttu, K. Y. Tan, I. Iisakka, R. Zhao, K. W. Chan, G. C. Tettamanzi, S. Rogge, A. S. Dzurak, and M. Möttönen, *Nano Lett.* **14**, 3405 (2014).
  - [14] M. R. Connolly, K. L. Chiu, S. P. Giblin, M. Kataoka, J. D. Fletcher, C. Chua, J. P. Griffiths, G. A. C. Jones, V. I. Falko, C. G. Smith, and T. J. B. M. Janssen, *Nature Nanotech.* **8**, 417 (2013).
  - [15] G. P. Lansbergen, Y. Ono, and A. Fujiwara, *Nano Lett.* **12**, 763 (2012).
  - [16] B. Roche, R.-P. Riwar, B. Voisin, E. Dupont-Ferrier, R. Wacquez, M. Vinet, M. Sanquer, J. Splettstoesser, and X. Jehl, *Nat. Commun.* **4**, 1581 (2013).
  - [17] G. Yamahata, K. Nishiguchi, and A. Fujiwara, *Nat. Commun.* **5**, 5038 (2014).

- [18] C. Tettamanzi, G., R. Wacquez, and S. Rogge, *New J. Phys.* **16**, 063036 (2014).
- [19] N. Feltin and F. Piquemal, *Eur. Phys. J. Spec. Top.* **172**, 267 (2009).
- [20] S. P. Giblin, S. J. Wright, J. D. Fletcher, M. Kataoka, M. Pepper, T. J. B. M. Janssen, D. A. Ritchie, C. A. Nicoll, D. Anderson, and G. A. C. Jones, *New J. Phys.* **12**, 073013 (2010).
- [21] S. P. Giblin, M. Kataoka, J. D. Fletcher, P. See, T. J. B. M. Janssen, J. P. Griffiths, G. A. C. Jones, I. Farrer, and D. A. Ritchie, *Nat. Commun.* **3**, 930 (2012).
- [22] A. Fujiwara and Y. Takahashi, *Nature* **410**, 560 (2001).
- [23] A. Fujiwara, N. M. Zimmerman, Y. Ono, and Y. Takahashi, *Appl. Phys. Lett.* **84**, 1323 (2004).
- [24] A. Fujiwara, K. Nishiguchi, and Y. Ono, *Appl. Phys. Lett.* **92**, 042102 (2008).
- [25] P. J. Koppinen, M. D. J. Stewart, and N. M. Zimmerman, *IEEE Trans. Electron Devices* **60**, 78 (2013).
- [26] K. Nishiguchi, A. Fujiwara, Y. Ono, H. Inokawa, and Y. Takahashi, *Appl. Phys. Lett.* **88**, 183101 (2006).
- [27] G. Yamahata, K. Nishiguchi, and A. Fujiwara, *Appl. Phys. Lett.* **98**, 222104 (2011).
- [28] L. Fricke, M. Wulf, B. Kaestner, V. Kashcheyevs, J. Timoshenko, P. Nazarov, F. Hohls, P. Mirovsky, B. Mackrodt, R. Dolata, T. Weimann, K. Pierz, and H. W. Schumacher, *Phys. Rev. Lett.* **110**, 126803 (2013).
- [29] L. Fricke, M. Wulf, B. Kaestner, F. Hohls, P. Mirovsky, B. Mackrodt, R. Dolata, T. Weimann, K. Pierz, U. Siegner, and H. W. Schumacher, *Phys. Rev. Lett.* **112**, 226803 (2014).
- [30] J. Bylander, T. Duty, and P. Delsing, *Nature* **434**, 361 (2005).
- [31] M. Seo, Y.-H. Ahn, Y. Oh, Y. Chung, S. Ryu, H.-S. Sim, I.-H. Lee, M.-H. Bae, and N. Kim, *Phys. Rev. B* **90**, 085307 (2014).
- [32] K. K. Likharev and A. B. Zorin, *J. Low Temp. Phys.* **59**, 347 (1985).
- [33] M. J. T. Milton, J. M. Williams, and A. B. Forbes, *Metrologia* **47**, 279 (2010).